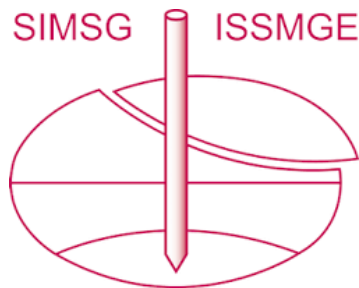


INTERNATIONAL SOCIETY FOR SOIL MECHANICS AND GEOTECHNICAL ENGINEERING



This paper was downloaded from the Online Library of the International Society for Soil Mechanics and Geotechnical Engineering (ISSMGE). The library is available here:

<https://www.issmge.org/publications/online-library>

This is an open-access database that archives thousands of papers published under the Auspices of the ISSMGE and maintained by the Innovation and Development Committee of ISSMGE.

The paper was published in the Proceedings of the 8th International Symposium on Deformation Characteristics of Geomaterials (IS-PORTO 2023) and was edited by António Viana da Fonseca and Cristiana Ferreira. The symposium was held from the 3rd to the 6th of September 2023 in Porto, Portugal.

Development of tools to investigate biocementation - microscale analysis for studying bacterial solutions

Mariana Pinto^{1#} and Rafaela Cardoso¹

¹CERIS/ Instituto Superior Técnico, Civil Engineering Department, Lisbon, Portugal

[#]corresponding author: mariana.mateus.pinto@gmail.com

ABSTRACT

Biocementation consists on the use of microorganisms (bacteria) to promote the precipitation of calcium carbonate (biocement). When this technique is applied in soils or fractured rocks, the biocement which is precipitated can fill voids and discontinuities, being easy to apply, not very intrusive and requiring low energy consumption. There are several aspects that must be investigated when using living microorganisms for such purpose, mainly related with ensuring the environmental conditions for their survival and the maximization of production of biocement. The age of the bacteria and the increment of biocement production after increasing the number of inoculations were investigated in the work presented in this paper. A microfluidic device was developed to visualize the production of biocement after multiple injections of bacteria and feeding solution. These devices allow for an easy and straight forward visualization of small-scale physical, chemical and biological processes. The results of injection cycles in microfluidics channel were examined with imaging techniques. In parallel, experimental tests were carried out on samples of uniform sand soil, with the objective of evaluating the penetration resistance and the calcium carbonate content that was formed, according to the number of injections. There was also a verification of the electrical conductivity of the bacterial solutions in use, to guarantee its viability. As expected, the production of biocement increased after three injections of bacteria, which is consistent with the results found in both microfluidic devices and soil samples.

Keywords: Biocement; Calcium Carbonate; Microfluidic device; Imaging Technique.

1. Introduction

The construction sector is one of the biggest responsible for high carbon emissions into the atmosphere (Chen *et al.* 2022). According to the Report of the Global ABC 2020 (Global Alliance for Buildings and Construction) of the United Nations Environment Programme, CO₂ emissions from the construction industry account for about 38% of total global CO₂ emissions. Thus, it is essential to continuously investigate methods and solutions, in association with the areas of sustainability and conservation, for the development of efficient construction technologies capable of reducing the energy involved in civil engineering projects.

In the field of biotechnological construction, the use of construction materials with less environmental impact in comparison to traditional methods can be made through the introduction of microorganisms in construction processes (Ivanov *et al.* 2015). The methods applied consist in the addition of microorganisms (bacteria or enzymes) and additives (Feeding Solution) capable of promoting the local formation of binder materials (biocement). These techniques involve natural chemical processes, which are less intrusive, present a lower energy consumption and contribute to the substantial improvement of larger area ranges, due to their low viscosity and injection pressure.

Nevertheless, this technique may present some limitations because it is energy intensive due to the feed

required and produces ammonia as a byproduct, which is harmful to the environment.

Evidence of the improvements that result from this method are the several possibilities of application that arise from it (e.g.: reduce soil permeability; increase strength of sands against liquefaction and erosion; capture of contaminants, immobilizing heavy metals; reduction of permeability in fractured rocks among others) (Dejong *et al.*, 2010; Mountassir, *et al.* 2014, Van Paassen *et al.* 2010, Phillips *et al.* 2013). Several research projects have shown that cracks filled with bacteria, nutrients and sand present a significant increase in compressive strength, stiffness and decreased permeability when compared to cases without bacteria (Siddique *et al.* 2011; Al-Thawad, S. 2011).

The risk of low biological activity may be insufficient to promote urea hydrolysis, a crucial domain for the development and application of this method in real environment conditions. In the context of soil stabilization, in a real setting, the injection of microorganisms may result in a non-homogeneous distribution or, possibly, in a scenario of competition or predation with native organisms, which difficult the creation of conditions and increases the study complexity in laboratorial environment (Phillips *et al.* 2013). Adding to that, expanding from laboratory scale to field scale is one of the largest challenges in this area (van Paassen *et al.* 2010) due to the large quantities necessary and homogeneity issues. In addition to the scale effects, the environmental and nutritional conditions of bacterial solutions and the dosages applied, contribute to the

success of the treatment (Whiffin 2004; Stocks-Fischer *et al.* 1999).

Soil behaviour and performance are directly related to micro or nano scale conditions. Recently, microfluidic devices have been used to monitor calcite precipitation in a controlled environment. Microfluidics devices allow the manipulation of small amounts of fluid, from the use of channels with dimensions from tens to hundreds of micrometers. One of the most recent methods of analysis corresponds to the use of microfluidic devices, due to their manufacturing versatility (flexible materials such as polymeric materials are usually used), their optical transparency and their extensive applicability, in particular in the investigation and visualization of small-scale physical, chemical and biological processes in the areas of chemical, biological, medical and environmental engineering (Pattanayak *et al.* 2021; Shu *et al.* 2022).

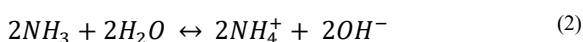
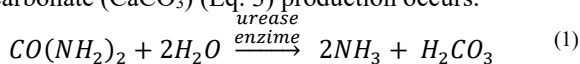
The introduction of microfluidic platforms in the study of micro-scale behaviour for geotechnical engineering applications is quite recent. Microscale experiments to verify calcium carbonate precipitation were performed by researchers to understand the influence of the variation of treatment procedures (for example, injection velocity, channels geometry, number of injections, injections strategies and others), relating CaCO_3 precipitation extension with the final size of the crystals, flow conditions and bacterial cell effects on precipitation (Wang *et al.* 2019).

In this paper, a microfluidic device was developed to visualize the production of biocement after three injections of bacteria and feeding solution. In parallel, experimental tests were carried out on samples of uniform sand soil, with the objective of evaluating the penetration resistance and amount of precipitated calcium carbonate content for this number of injections. The results found in both tests were compared for validation of the visualization process adopted.

2. MICP process (Microbiologically Induced Calcite Precipitation)

The biomineralization process using bacteria is usually called Microbiologically Induced Calcite Precipitation (MICP). Its occurrence is dependent on three main components: urea source ($\text{CO}(\text{NH}_2)_2$), calcium source (usually calcium chloride, CaCl_2) and the intervention of the urease enzyme. The urease enzyme can be found in a wide range of microorganisms and plants. The most applicable biological agents in civil engineering are represented by bacteria, and the most used bacterial species is *Sporosarcina Pasteurii*, of nonpathogenic character and with a high production capacity of urease.

MICP initiates with the intervention of the urease enzyme, responsible for hydrolysis of urea in ammonia and carbonic acid (Eq.1). The existence of ammonia and the pH increase allows the production of OH^- ions (Eq. 2). In the presence of calcium ions (CaCl_2), calcium carbonate (CaCO_3) (Eq. 3) production occurs.



Calcium carbonate can present three crystal forms: calcite (more stable carbonate under environmental conditions), aragonite (high pressure carbonate) and vaterite (unstable hydrated carbonate) (Al-Thawad 2011). Calcite is intended, but vaterite is usually found in a secondary, metastable or transitional phase in the formation of calcite (Phillips *et al.* 2013). One of the main challenges in optimizing the MICP process corresponds to the type of crystal formed, compromising the effectiveness of the treatment and its durability (case of vaterite, of unstable nature) (Ivanov *et al.* 2015).

3. Microfluidic device

3.1. Description of the device

To evaluate the MICP process in small-scale fractures, microfluidic devices with controlled-size channels were used. The structures allowed for a detailed observation of the phenomena depending on the number of injections performed. For this purpose, a structure composed of 2 acrylic plates (50 x 24 mm), with a thickness of 3 mm each and a 2 mm wide channel, manufactured through a CNC Milling Machine, was dimensioned. Each end of the channel had a corresponding inlet and outlet built, at the entrance and exit of the fluid in the system. The parts were coupled with 6 steel screws (M3 x 10 mm), and an rubber seal was installed to make sure that the manufactured channels were properly sealed. Later, connectors were manufactured to attach to the water inlet and outlet channels as to ensure a controlled, leak-free injection process. The size of the channel was designed following similar experiments by Mountassir *et al.* (2014)

Fig. 1 shows a schematic representation of the projected plates and Fig. 2 shows the final configuration of the plate and its elements.

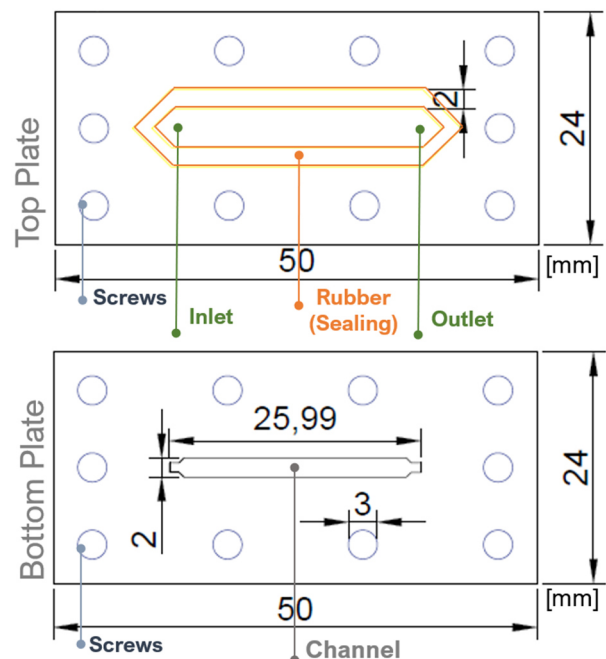


Figure 1. Schematic representation of the top and base plates.

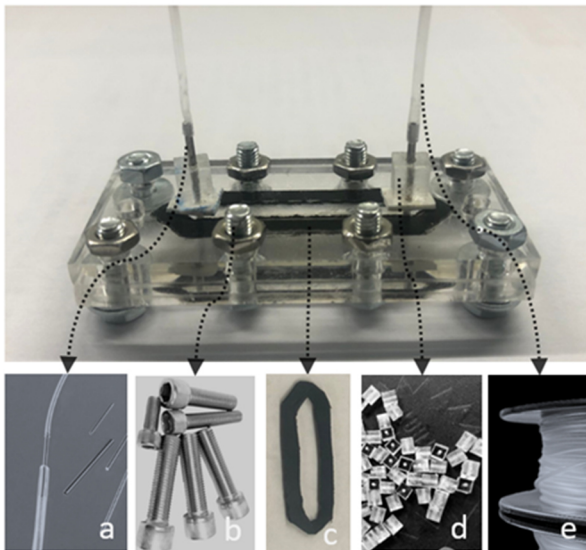


Figure 2. Final plate configuration. a. Metal connecting tubes (\varnothing 0.8 mm; length: 15 mm); b. Screws M3 x 10 mm; c. rubber seal, e:1 mm; d. Connectors (0.4 x 0.4 mm); e. Polyethylene tube (PE-60, fits 20 ga, 0.03 x 0.048 in).

3.2. Microscope Visualization

The tests performed consisted in injecting bacteria, followed by injecting feeding solution after 5 minutes (52 μ L of each). The channel was completely filled and the precipitation of biocement was monitored and recorded by an optical microscope (AmScope) that allows the capture of video and digital imaging (Fig. 3).

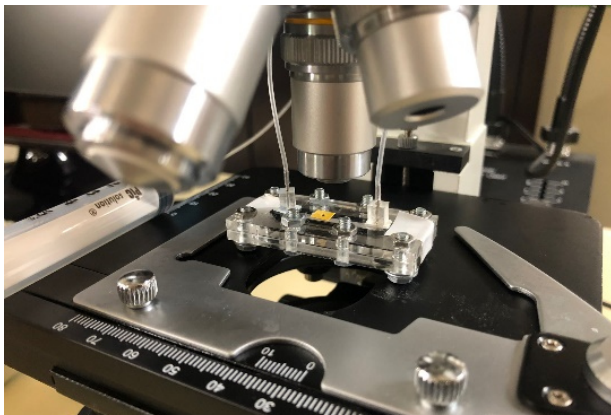


Figure 3. Visualization of the microfluidics device under the optical microscope.

The images captured during the tests were processed using the ImageJ processing and analysis *software*. Specific tools were used to identify and quantify areas of formed biocement. Fig. 4 shows a process schema of the process adopted to define its quantification.

The quantification of the amount of precipitated biocement is done by applying the threshold function, creating binary images that make it possible to identify areas with calcium carbonate. The quantity of biocement can be quantified as the percentage of area of the pixels corresponding to biocement in the total area analysed, using Eq. 4.

$$\%Area CaCO_3 = \frac{\text{area of biocement}}{\text{total area}} \times 100 \quad (4)$$

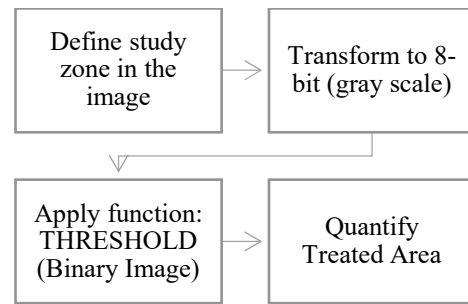


Figure 4. Image treatment process for quantification of calcium carbonate formed.

4. Liquid Samples

4.1. Bacteria and feeding solution

The bacteria species adopted were *Sporosarcina pasteurii* from American Type Culture Collection (ATCC Strain 11859, American Type Culture Collection). The bacteria concentration adopted for the treatments was $\sim 10^8$ cells/mL. The feeding solution was prepared with urea (0.5 M) and calcium chloride (0.5 M).

4.2. Urease activity through electrical conductivity

The urease activity helps to understand if bacteria are alive, because it measures the consumption of urease enzyme in a fluid where both bacteria and urea are present in controlled quantities. The electrical conductivity presents a linear increase due to MICP reactions, producing ammonium ions. The solution becomes more conductive due to the presence of ammonium ions (positively charged), resulting from the hydrolysis of urea. Consequently, the concentration of ionic products is proportional to the conductivity of the solution. In this paper it was measured for the fresh bacteria to confirm their viability.

The experiment was carried out following the protocol defined by Harkes (2009). For this, 0.5 mL of the culture was added to test tubes containing 4.5 mL of urea solution (1.1 M), followed by homogenization. Measurements were performed every minute, in an interval of 5 minutes using a conductivity meter (Crison MM41). The conductivity variation rate ($\text{mS} \cdot \text{cm}^{-1} \cdot \text{min}^{-1}$) was determined by the slope of the linear regression line of conductivity measurements along time. As defined by Harkes, (2009), an increase of 1mS in urease solution is equivalent to the hydrolysis of 11mM urea/min.

5. Methodology

5.1. Sand used and soil sample preparation

The samples were prepared in cylindrical flasks ($r=1.5$ cm) with a drainage base layer, formed by gravel ($D_{50}=3$ mm) with a height of 0.5 cm. The soil used was a uniform grading sized sand (Reference: APAS 30) with a height of 2 cm, placed above the base layer. An orifice (Outlet) of 0.5 cm in diameter was carved in the base layer to allow the flow of the injected fluid into the

samples and its consequent extraction. The two layers were separated by a filter paper (Fig. 5).



Figure 5. Photograph of a soil sample.

According to the unified soil classification, APAS 30 sand is a poorly graded sand (SP) with quartzite, quartz and feldspar minerals. The mean diameter of particles is $D_{50} = 0.3$ mm and the uniformity coefficient (C_u) is 2 (Rodríguez, et al., 2022). The volumetric weight of solid particles is 26.8 kN/m^3 . The samples were prepared to have void ratio $e = 0.78$, which corresponds to a dry volumetric weight of 15 kN/m^3 .

The treatment fluids were injected in the soil surface and the treatment was repeated for three days (I-one injection, II-two injections and III-three injections) (Fig. 6). One injection was applied each day, with the following quantities: 1/3 void volume of distilled water, 1/3 void volume of bacterial solution and 1/3 void volume of feeding solution.

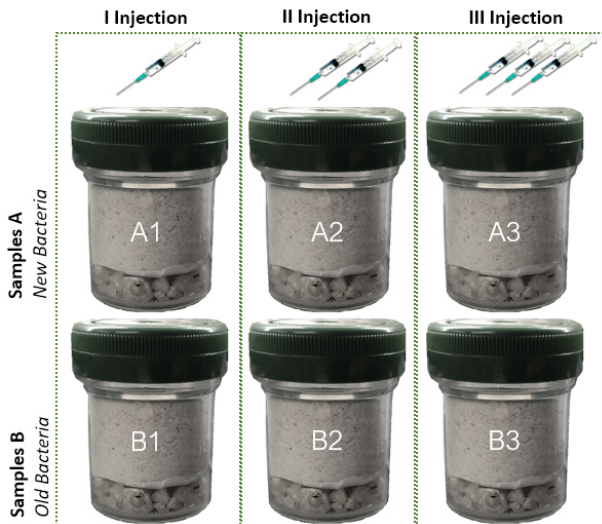


Figure 6. Example of testing strategy.

The tests were carried out on 6 sand samples (A1 to A3; B1 to B3), for each number of injections. The difference between the samples A and B is the age of the bacteria used. Bacteria A were injected still fresh, while bacteria B were 6 days old, being stored in the fridge prior to its injection into the soil.

5.2. Penetrometer Test

The treated sand samples were tested with penetrometers (CONTROLS Geopocket dial penetrometer, model 16-T0161). This equipment allowed

for a quick determination of the penetration strength (Fig. 7). Its readings are determined through the pressing of the plunger into the soil, up to the groove line. The plunger used has a 6.4 mm in diameter and a inner dial scale that ranges from 0 to 6.0 kg/cm^2 . The surface of the soil samples was flattened as much as possible, to reduce error in this test and strength was measured in a full saturation state.



Figure 7. Penetrometer used for the tests (CONTROLS Geopocket).

5.3. Carbonate content in sand samples

The calcium carbonate content was determined by a leaching test, using hydrochloric acid (HCl, 0.5M). The dissolution of calcium carbonate results in solid mass loss (Fig. 8). The percentage of calcium carbonate is the relation between the dry mass lost and the initial dry mass (Eq. 5), where m_1 corresponds to the initial dry sand mass and m_2 to the dry sand mass after the leaching test.

$$\%CaCO_3 = \frac{m_1 - m_2}{m_1} \times 100 \quad (5)$$



Figure 8. Leaching test to determine calcium carbonate content.

6. Results and discussion

6.1. Urease activity to check the viability of bacteria

The activity of the fresh bacteria used in both microfluidic device and soil was measured after being injected for the first time. The evolution of electrical conductivity measured along time is presented in Fig. 9. Based on the results, the bacterial solution used throughout the tests presented a hydrolyzed urea value of $6.73 \text{ mM urea/hour}$ for a slope of 0.0102 mS/cm/min . This confirms that the bacteria in use are viable for the study.

The urease activity was measured by Cardoso et al. (2023) along several days for different lots of bacteria. It was possible to confirm that this bacteria species maintains urease activity for 6 days, followed by a fast reduction at the end of 10 days of age. This determined the time interval chosen for this study.

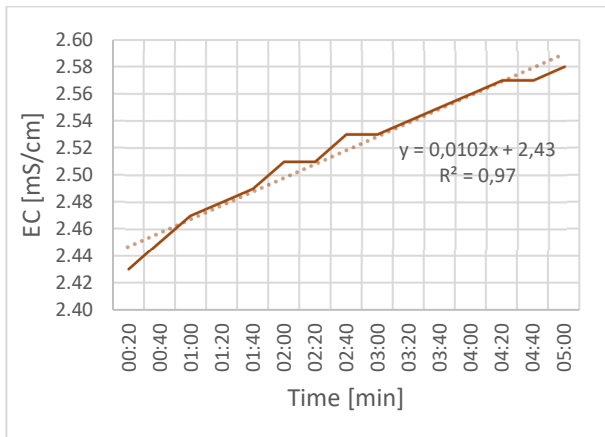


Figure 9. Variation of electrical conductivity over time for the fresh bacteria used.

6.2. Microscope Visualisation of Microfluidic Device

Fig. 10 shows the images of the microfluidic channel captured by the optical microscope throughout the various injections (I, II and III) and their treatment performed with the ImageJ software.

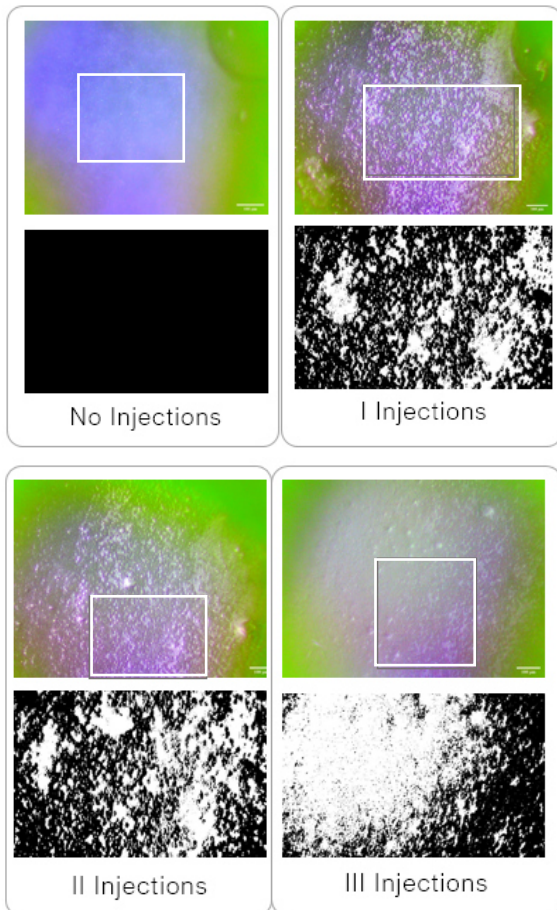


Figure 10. Images captured in the microfluidic channel with 0, I, II and III injections and respective image processing result (Binary Image). The white zones correspond to the biocement.

The zones of the channel observed in the microscope selected were defined by using a rectangular yellow sticker with a circular opening, presented in Fig. 3. Only the inner zone of this marker were analysed, identified with a square in Fig. 10. The processed images were converted in binary images (white or black pixels) when

the Threshold functionality was applied. The white spots in the binary images represent the areas where biocement is present.

It is possible to observe that the areas where the white spots concentrate increase in size with an increasing number of injections. A functionality was applied over the treated images, which allowed to quantify the areas with the presence of biocement (white pixels) in the total area observed. The percentage of biocement was computed using Eq. 4 previously presented. The results are presented in Fig. 11, where it is possible to observe the increment of carbonate formation according to an increasing number of injections. The value found for the last injection, however, has some negative influence on the photography of light reflections.

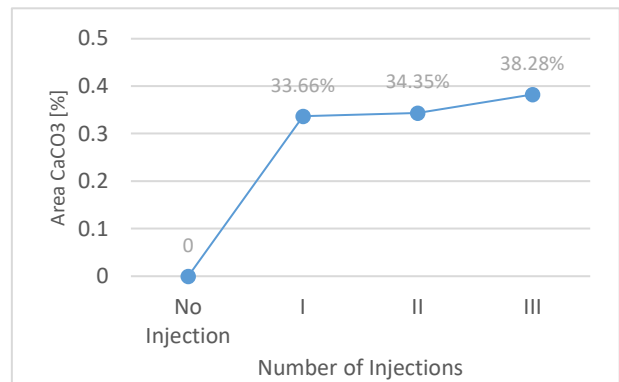


Figure 11. Amount of calcium carbonate formed as a function of the number of injections.

6.3. Penetrometer Test

Through the tests with the penetrometer on the treated sand samples, an increase in the penetration strength was observed, which is a result of the increased number of injections (Fig. 12). The values measured in samples A are higher than those measured in samples B. This was already expected considering the age of the bacteria and the experience on the evolution of urease activity along large periods of time. All results were higher or equal to the control sample, saturated with water (20 kPa).

Independently from the age of the bacteria, the penetration strength measured continued increasing with increasing number of injections, being the highest values measured for the samples treated with three injections (samples III). This indicates that biocement continued to precipitate. The increment observed along time followed similar paths for both samples A and B. The strength measured at the end of three injections for samples A was 8 times bigger than the one measured after one injection, while for samples B it was 7.5 times bigger than the one measured after one injection. Nevertheless, the strength measured in samples A was larger than that measured in samples B (except after the second injection), which may be explained by the largest activity of fresh bacteria.

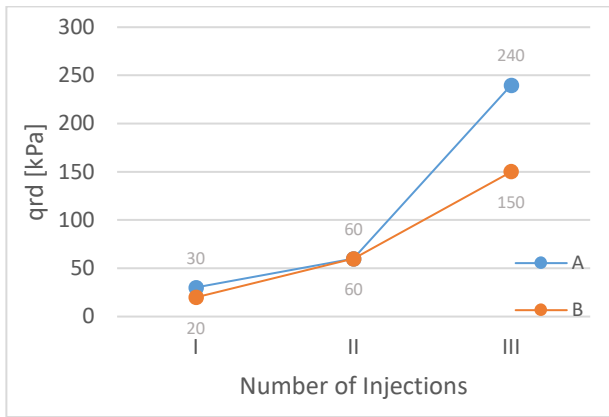


Figure 12. Results of penetration strength with the number of injections.

6.4. Carbonate content in sand samples (%CaCO₃)

Fig. 13 shows the values of the calcium carbonate content precipitated after one, two and three injections. As expected, and in accordance with the penetration strengths measured, the calcium carbonate content increased with the number of injections, reaching values of 3.78% in samples A and 2.54% in samples B after the third injection. As for the compression strength, the differences of the final values for samples A and B are associated to the age of bacteria. The ultimate difference is in the final amount of calcium carbonate content, which is 1.24%.

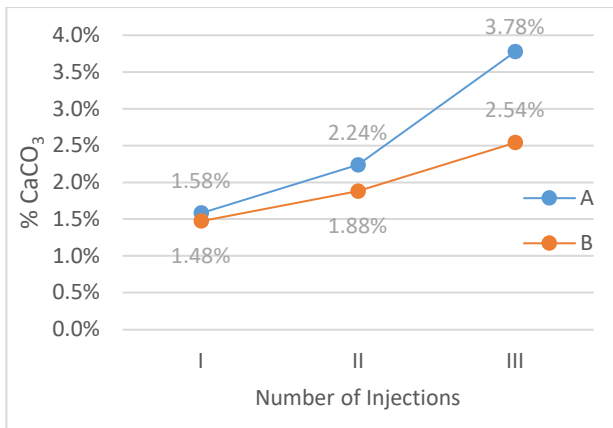


Figure 13. Content of calcium carbonate with the number of injections.

6.5. Joint analysis of the results

The results found in visual observations using the microfluidic device and in the soil samples are consistent, as both confirm that the amount of biocement precipitated has increased according to the increase of the number of injections. The relation between the penetration strength and the percentage of calcium carbonate for samples A and B is presented in Fig. 14. Both samples fit perfectly the same linear relationship, which confirms that this strength is caused by the presence of precipitated calcium carbonate. Although the age of bacteria influences the amount of biocement precipitated, and therefore the final compression strength achieved, the treatment remains viable for the age

interval which was considered. The linear relationship will also be valid for a limited interval.

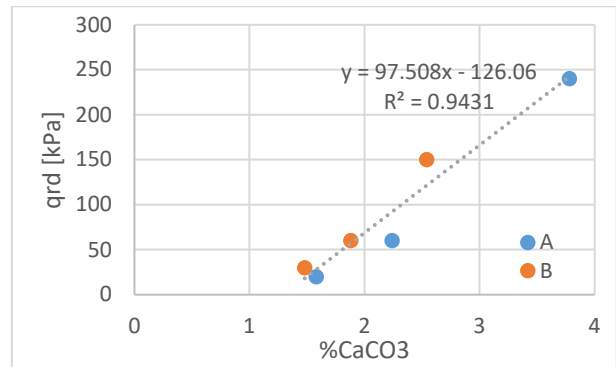


Figure 14. Relationship between the calcium carbonate and penetration strength.

7. Conclusions

A microfluidic device was used in this study to visualize the precipitation of biocement for three successive injections of bacteria. As expected, a higher number of injections determined an increase of the formation of precipitate, observed through the use of this device and also in the parallel tests performed in the soil samples. The values of penetration strength and carbonate content also increased with a growing number of injections. Similar paths were observed in the soil samples for the different ages of bacteria tested, probably because the oldest bacteria were still viable.

This study and the development of small-scale MICP visualization platforms was important to understand the visualization techniques in terms of dimensions, light, sealing and injection forms in the microfluidic device. The experiments using microfluidics devices will allow to assess the conditions on a microscale and to understand the influence of the treatment method adopted, related to the extent of precipitation of CaCO₃. The identification of treatment conditions such as the dosages adopted and the period of application after the manufacture of bacteria is of utmost importance for understanding the precipitation mechanisms and optimizing this treatment.

Acknowledgements

The authors acknowledge INESC-MN for the help building the microfluidic device used, and FCT I.P for the funding through PhD individual grant ref. 2020.09111.BD and research project CALCITE, ref. PTDC/ECI-EGC/1086/2021.

References

- Al-Thawad, S. Ureolytic Bacteria and Calcium Carbonate Formation as a Mechanism of Strength Enhancement of Sand, *Journal of Adv. Sc. and Eng. Research* 1, pp. 98-114, 2011, <https://www.researchgate.net/publication/230603500>
- Cardoso, R., Vieira, J. and Borges, I. (2023). On the use of Biocementation to treat collapsible soils. *Engineering Geology*, 313, 106971, <https://doi.org/10.1016/j.enggeo.2022.106971>

- Chen, J., Shi, Q., Zhang, W. Structural path and sensitivity analysis of the CO₂ emissions in the construction industry, *Environmental Impact Assessment*, Volume 92, pp. 1 – 2, 2022, <https://doi.org/10.1016/j.eiar.2021.106679>
- DeJong, J. T., Mortensen, B. M., Martinez, B. C., Nelson, D. C., Bio-mediated soil improvement, *Ecological Eng.*, Volume 36, pp. 197-210, 2010, <https://doi.org/10.1016/j.ecoleng.2008.12.029>
- Harkes, M., Van Paassen, L., Booster, J., Whiffin, V., Loosdrecht, C. M. Fixation and distribution of bacterial activity in sand to induce carbonate precipitation for ground reinforcement, *Ecological Eng.*, Volume 36, pp. 112-117, 2009, [doi:10.1016/j.ecoleng.2009.01.004](https://doi.org/10.1016/j.ecoleng.2009.01.004)
- Ivanov, V., Chu, J., Stabnikov, V. Basics of construction microbial biotechnology, In: *Biotechnologies and Biomimetics for Civil Engineering*, 1st ed., Springer Cham, Switzerland, 2015, pp. 21-56, <https://doi.org/10.1007/978-3-319-09287-4>
- Mountassir, G., Lunn, R., Moir, H., Maclachlan, E. Hydrodynamic Coupling in Microbially Mediated Fracture Mineralization: Formation of Self-Organized Groundwater flow channels. *Water Resources Research*, Volume 50, pp. 1-16, 2014, <https://doi.org/10.1002/2013WR013578>
- Pattanayak, P., Kumar Singh, S., Gulati, M., Vishwas, S., Kapoor, B., Chellappan, D. K., Anand, K., Gupta, G., Jha, N.K., Gupta, P. K., Prasher, P., Dua, K., Dureja, H., Kumar, D., Kumar, V. Microfluidic chips: recent advances, critical strategies in design, applications and future perspectives, *Microfluidics and Nanofluidics*, pp. 1 - 28, 2021, <https://doi.org/10.1007/s10404-021-02502-2>.
- Phillips, A., Gerlach, R., Lauchnor, E, Mitchell, A., Cunningham, A., Spangler, L. Engineered applications of ureolytic biomineralization: A review, *Biofouling*, Volume 29, pp. 715-733, 2013, <https://doi.org/10.1080/08927014.2013.796550>
- Rodríguez, R., Cardoso, R. Study of biocementation treatment to prevent erosion by concentrated water flow in a small-scale sand slope, *Transportation Geotechnics*, Volume 37, 2022. <https://doi.org/10.1016/j.trgeo.2022.100873>.
- Shu, S., Shuang, Chen, H., Meng, H. (2022). Modelling Microbially Induced Carbonate Precipitation (MICP) in Microfluidic Porous Chips. *Hindawi Geofluids*, pp. 1 – 8, Volume 2022, <https://doi.org/10.1155/2022/3616473>.
- Siddique, R., and N. K. Chahal. Effect of ureolytic bacteria on concrete properties, *Construction and Building Materials*, Volume.25, pp. 3791-3801, 2011, <https://doi.org/10.1016/j.conbuildmat.2011.04.010>
- Stocks-Fischer, S.; Galinat, J. K.; Bang, S. Microbiological precipitation of CaCO₃, *Soil Biol. Biochem.*, Volume 31, pp. 1563-1571, 1999, [https://doi.org/10.1016/S0038-0717\(99\)00082-6](https://doi.org/10.1016/S0038-0717(99)00082-6)
- United Nations Environment Programme (2020). *Global Status Report for Buildings and Construction: Towards a Zero-emission, Efficient and Resilient Buildings and Construction Sector*. Nairobi
- Van Paassen, L., Ghose, R., Linden T., Van der Star W., Loosdrecht, M. Quantifying Biomediated Ground Improvement by Ureolysis: Large-Scale BiogROUT Experiment, *Journal of Geotech. and Geoenv. Eng.*, Volume 136, 1721-1728, pp. 1721-1728, 2010, [10.1061/\(ASCE\)GT.1943-5606.0000382](https://doi.org/10.1061/(ASCE)GT.1943-5606.0000382)
- Wang, Y., Soga, K., DeJong, J T., Kabla, A. Microscale Visualization of Microbial-Induced Calcium Carbonate Precipitation Processes, *J. of Geotech. and Geoenv. Eng.*, 04019045, 145(9), 2019, [DOI: 10.1061/\(ASCE\)GT.1943-5606.0002079](https://doi.org/10.1061/(ASCE)GT.1943-5606.0002079)
- Wang, Y., Soga, K., Dejong, J T., Kabla, A., A Microfluidic Chip and its use in Characterising the Particle-Scale Behaviour of Microbial-Induced Calcium Carbonate Precipitation (MICP), *Geotechnique*, Volume 69, pp. 1086-1094, 2019, <https://doi.org/10.1680/jgeot.18.P.031>
- Whiffin, V. S. Microbial CaCO₃ Precipitation for the Production of Biocement. PhD thesis Philosophy in Biotechnology. Murdoch University, Western Australia, 2004: <https://researchrepository.murdoch.edu.au/id/eprint/399/2/02Whole.pdf> [Accessed: april 2022]